Journal of Alloys and Compounds 506 (2010) 766–771

Contents lists available at ScienceDirect

Journal of Alloys and Compounds

journal homepage: www.elsevier.com/locate/jallcom

Effects of Fe substitution on structural and magnetic properties of the $Nd_2Co_{7-x}Fe_x$ compounds

YuQi Yang, G.H. Rao*, T. Wang, J.B. Li, J. Luo, G.Y. Liu, X.J. Chen, J.L. Zhao

Beijing National Laboratory for Condensed Matter Physics, Institute of Physics, Chinese Academy of Sciences, Beijing 100190, China

ARTICLE INFO

Article history:
Received 13 May 2010
Received in revised form 4 July 2010
Accepted 7 July 2010
Available online 15 July 2010

Keywords:
$Nd_2Co_{7-x}Fe_x$
Crystal structure
Spin-reorientation
Magnetic phase diagram

ABSTRACT

The structural and magnetic properties of the $Nd_2Co_{7-x}Fe_x$ compounds related to $R_{m+n}T_{2m+5n}$ series (R = rare earth, T = transition metal) were investigated by means of X-ray diffraction and magnetic measurements. The compounds crystallize in the Ce_2Ni_7-type structure with the space group $P6_3/mmc$ between $x = 0.0$ and 2.1. For higher Fe content the $Nd_2(CoFe)_7$ either coexists with the $Nd(CoFe)_3$ phase ($x > 2.1$) or decomposes to $Nd(CoFe)_3 + Nd_2(CoFe)_{17}$ ($x > 2.4$). The single phase $Nd_2Co_{7-x}Fe_x$ compounds exhibit two spin-reorientation transitions (SRT) for $x < 1.5$. The substitution of Fe for Co elevates both the spin-reorientation transition temperatures for $x < 1.5$ and finally leads to a single ferromagnetism to paramagnetism transition for $x \geq 1.5$. A magnetic phase diagram is constructed based on the magnetic measurements, thermogravimetry analysis under a low magnetic field and X-ray diffraction of magnetically aligned samples. The saturation magnetization of the compounds increases gradually first with the Fe content for $x \leq 0.20$, substantially for $0.20 < x < 1.5$, and then decreases for $x > 1.5$, which can be elucidated by a depletion effect of d band electrons due to the substitution of Fe for Co and the spin-flipping due to an enhanced d band splitting.

1. Introduction

The rare earth cobalt compounds with the hexagonal Ce_2Ni_7-type structure or the rhombohedral Gd_2Co_7-type structure belong to a structural series $R_{m+n}T_{2m+5n}$ (R = rare earth atoms, T = transition metal atoms), which is composed of m layers of Laves-phase RT_2 slabs and n layers of $CaCu_5$-type slabs stacking alternately along the *c* direction [1]. The stacking of the slabs is accompanied by a shift of the layers that gives rise to either a hexagonal or a rhombohedral symmetry [2,3]. With high magnetocaloric effect (MCE) of the Laves-phase RCo_2 at low temperature [4–7] and high saturation magnetization of $CaCu_5$-type phase at high temperature, $R_{m+n}T_{2m+5n}$ compounds might be promising MCE candidates for applications around ambient temperature.

The binary compound Nd_2Co_7 ($m = 2, n = 2$) is stable in the Nd–Co system and crystallizes in the hexagonal Ce_2Ni_7-type structure with the space group $P6_3/mmc$. Andreev et al. [8] and Bartashevich et al. [9] reported that the magnetic structure of Nd_2Co_7 experienced two fluctuations as temperature increases: a spin-reorientation (SR) occurred around 225 K and another SR around 290 K, with an alteration of the easy magnetization direction (EMD) from *a*-axis below the first SR transition to the *c*-axis above the second SR transition. However, binary "R_2Fe_7" does not exist possibly due to much higher mixing enthalpy between R and Fe than that between R and Co [10]. In addition, Co and Fe atoms on the same crystallographic position in a rare earth transition metal intermetallic compound usually exhibits opposite sign of magnetocrystalline anisotropy and different ferromagnetic character (strong vs. weak ferromagnetism). Therefore, an exploration of new members of the $R_{m+n}T_{2m+5n}$ family with Fe element is of significance for enriching our understanding of rare earth transition metal intermetallic compounds. In this paper we report crystal structure and magnetic properties of $Nd_2Co_{7-x}Fe_x$ compounds. Special attention will focus on the solubility limit of Fe and the influence of Fe atom on the structure, magnetic properties and spin-reorientation transitions (SRT) of the compounds.

2. Experimental details

Alloys with the composition $Nd_2Co_{7-x}Fe_x$ ($x = 0.0$–4.0) were prepared by arc-melting metal ingots of Nd, Co and Fe (purity >99.98% for Fe and Co, >99.9% for Nd) in an argon atmosphere. All alloys were remelted at least four times to ensure homogeneity. The alloy ingots were wrapped in Ta foil, sealed into evacuated quartz tubes and annealed one week in vacuum at 1353 K for $x = 0.0$–1.0, at 1303 K for $x = 1.0$–2.0, and at 1263 K for $x = 2.0$–4.0, respectively, then furnace-cooled to room temperature.

The samples were examined by means of X-ray powder diffraction (XRD) and thermo-magnetic analysis. The XRD data were collected on a Rigaku D/max-2500 diffractometer with Cu Kα radiation and a graphite monochromator. The XRD data used for structure refinement were collected in a step-scan mode with a sampling

* Corresponding author at: Beijing National Laboratory for Condensed Matter Physics, Institute of Physics, Chinese Academy of Sciences, Beijing 100190, China.
E-mail addresses: yangyuqi5@gmail.com (Y.Q. Yang), ghrao@aphy.iphy.ac.cn (G.H. Rao).

0925-8388/$ – see front matter © 2010 Elsevier B.V. All rights reserved.
doi:10.1016/j.jallcom.2010.07.065

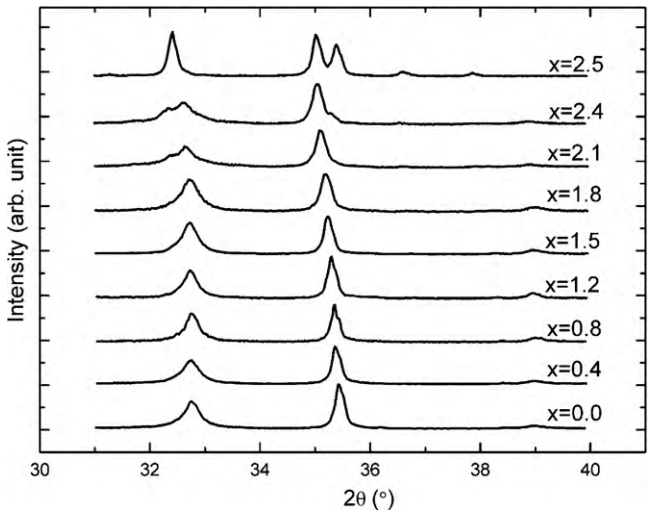

Fig. 1. XRD patterns of $Nd_2Co_{7-x}Fe_x$ ($0 \le x \le 2.5$).

time of 3 s and a sampling step of 0.02° in the 2θ range of 18–120°. Temperature dependence of magnetization of the samples was measured under a field of 1 kOe with a vibrating-sample magnetometer (VSM) from room temperature to above the Curie temperature. The ac magnetic susceptibility below 300 K of the samples was measured by a mutual inductance bridge at a fixed frequency of 320 Hz. Field dependence of magnetization of the samples was measured on a SQUID magnetometer at 5 K in magnetic fields up to 70 kOe, and the saturation magnetization was derived according to the law of approach to saturation. The Curie temperature was determined based on thermogravimetry analysis (SDT Q600 TA Instrument) under a low magnetic field exerted by a permanent magnet. The easy magnetization direction of the samples at room temperature was identified on the basis of the XRD pattern of magnetically pre-aligned specimens, which were prepared by solidifying a mixture of fine alloy particles with epoxy resin at room temperature in a field of about 10 kOe perpendicular to the specimen surface.

3. Results and discussion

3.1. Crystal structure

Portions of the XRD patterns of the $Nd_2Co_{7-x}Fe_x$ are shown in Fig. 1 for phase identification. The sample is single phase and crystallizes in the Ce_2Ni_7-type structure (space group $P6_3/mmc$) for $x = 0.0$–2.1. With the increase of the Fe content, the intensity of a shoulder peak at $2\theta \sim 32.5°$ increases for $x = 2.1$–2.5 (Fig. 1), indicating an increasing amount of the RT_3 phase (also a member of $R_{m+n}T_{2m+5n}$-type compounds with $m = 2$ and $n = 1$). For the sample with $x = 2.5$, the 2:7 phase disappears completely and decomposes to $Nd(CoFe)_3 + Nd_2(CoFe)_{17}$. The lattice parameters of the compounds were derived by profile decomposition and listed in Table 1. Fig. 2 shows the composition dependence of lattice constants for the $Nd_2(CoFe)_7$ phase ($x < 2.5$), the $Nd(CoFe)_3$ phase ($x \ge 2.5$) and the $Nd_2(CoFe)_{17}$ phase (inset). For the 2:7 phase, the lattice parameter a increases linearly with the Fe content, whereas the lattice parameter c decrease slightly.

Table 1
Lattice parameters a and c, Curie temperature T_C, saturation magnetization M_S at 5 K, and the EMD at room temperature for $Nd_2Co_{7-x}Fe_x$ compounds.

x	a (Å)	c (Å)	T_C (K)	EMD	M_S (μ_B/f.u.)
0.0	5.0648(2)	24.4652(7)	605.2	c-Axis	13.60
0.2	–	–	622.2	c-Axis	13.82
0.4	5.0702(1)	24.4413(8)	638.8	Cone	14.24
0.6	–	–	652.5	Cone	14.64
0.8	5.0809(2)	24.4233(7)	666.6	Planar	14.98
1.0	5.0898(1)	24.4517(8)	680.3	Planar	15.85
1.2	5.0914(3)	24.4321(11)	689.2	Planar	16.34
1.4	5.0968(2)	24.4301(7)	698.4	Planar	17.06
1.5	5.1010(3)	24.4486(12)	701.4	Planar	17.17
1.8	5.1063(2)	24.4307(11)	714.1	Planar	16.98
2.1	5.1093(3)	24.4238(13)	725.1	Planar	–
2.4	5.1155(2)	24.4308(13)	730.3	Planar	–

The crystal structure of the single phase $Nd_2Co_{7-x}Fe_x$ was refined by the Rietveld technique, using the refinement program Rietan 2000 [11]. Fig. 3 displays the experimental and calculated XRD patterns as well as the difference between them for Nd_2Co_7 and $Nd_2Co_{5.5}Fe_{1.5}$. The atomic parameters for some selected compounds, Nd_2Co_7, $Nd_2Co_{6.2}Fe_{0.8}$ and $Nd_2Co_{5.5}Fe_{1.5}$, were listed in Table 2.

Because Fe has a larger atomic radius than Co, an expansion of lattice is expected with the increasing substitution of Co by Fe. Based on the refined structural parameters, the thicknesses of the $Nd(CoFe)_5$ slabs and the $Nd(CoFe)_2$ slabs along the c direction in $Nd_2Co_{7-x}Fe_x$, i.e. the interplanar distance between atomic layer of the atoms on the 12k sites, can be calculated. With the increase

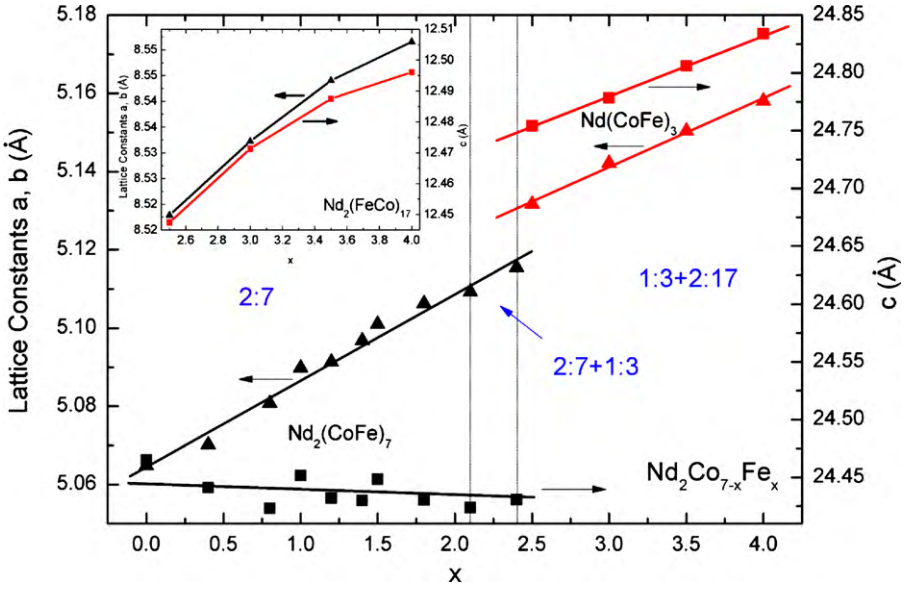

Fig. 2. The composition dependence of lattice constants of $Nd_2Co_{7-x}Fe_x$. 2:7 phase for $x < 2.5$, 1:3 phase and 2:17 phase (inset) for $x \ge 2.5$. The 2:7 phase and 1:3 phase coexist for $2.1 < x < 2.5$, and the 1:3 phase and 2:17 phase coexist for $2.5 \le x \le 4$.

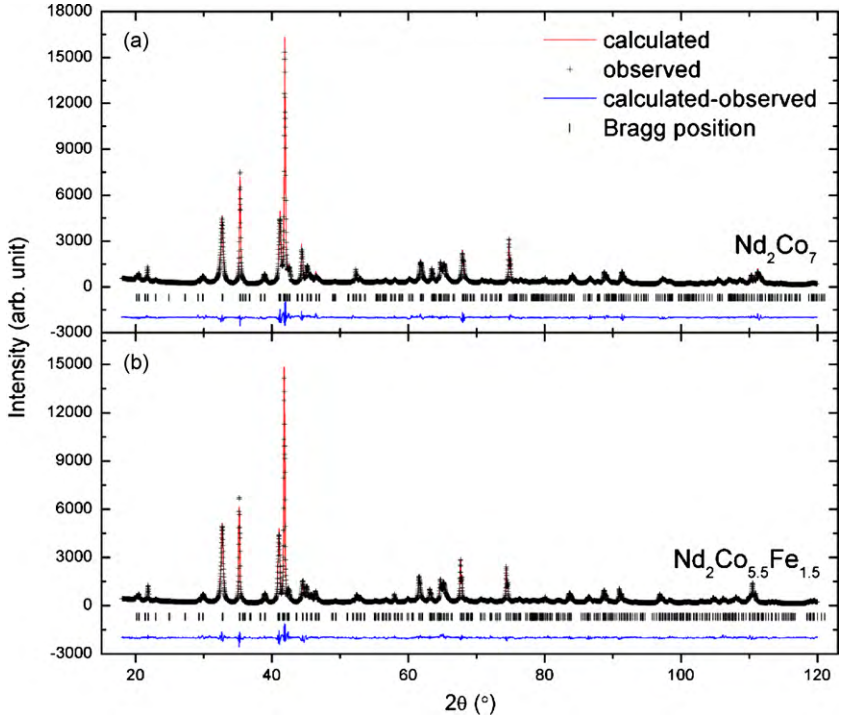

Fig. 3. Observed and calculated XRD patterns of the compound Nd_2Co_7 (a) and $Nd_2Co_{5.5}Fe_{1.5}$ (b). In each graph, the lowest curve is the difference between the observed and the calculated intensities, and the vertical bars at the bottom indicate Bragg reflection positions.

of the Fe content, the thickness of the $Nd(CoFe)_5$ slabs increases, whereas the thickness of the $Nd(CoFe)_2$ slabs decreases, leading to the observed slight reduction of the *c*-axis in $Nd_2Co_{7-x}Fe_x$. Therefore, it seems that the substitution of Fe for Co results in an expansion of the $Nd(CoFe)_5$ slabs along all three directions as in $Nd(Co_{0.95}Fe_{0.05})_5$ and $Y(Co_{1-x}Fe_x)_5$ compounds [12–14] and causes a shrinkage of the $Nd(CoFe)_2$ slabs. The shrinking of the $Nd(CoFe)_2$ slabs coincides with the fact that the $NdFe_2$ compound was stabilized under a high pressure [15].

For the $CaCu_5$-type structure, it was reported that the large Fe atoms occupied preferentially the 3g site in $Nd(Co_{0.95}Fe_{0.05})_5$ and $Y(Co_{1-x}Fe_x)_5$ [12–14]. The 3g sites in the $CaCu_5$-type structure form a kagomè lattice and correspond to the 6 h and the 12k sites in the Nd_2Co_7 structure. It is likely that the Fe atoms also preferentially reside on the kagomè lattice in $Nd_2Co_{7-x}Fe_x$, i.e. the 6 h and the 12K sites. Neutron diffraction experiments are desirable to determine the distribution of the Fe atoms over the five crystallographically inequivalent positions.

Table 2
Rietveld refinement results of the crystal structure of $Nd_2Co_{7-x}Fe_x$, space group $P6_3/mmc$. Co1 at 2a (0,0,0).

$Nd_2Co_{7-x}Fe_x$	$x=0.0$	$x=0.8$	$x=1.5$
Lattice constants			
a (Å)	5.0648(2)	5.0809(2)	5.1010(3)
c (Å)	24.4652(7)	24.4233(7)	24.4486(12)
Atomic positions			
Nd1: 4f(1/3,2/3,*z*), *z*	0.0268(1)	0.0269(2)	0.0268(2)
Nd2: 4f(1/3,2/3,*z*), *z*	0.1721(2)	0.1717(1)	0.1719(2)
Co2: 4e(0,0,*z*), *z*	0.1736(4)	0.1708(3)	0.1724(5)
Co3: 4f(1/3,2/3,*z*), *z*	0.8338(3)	0.8320(3)	0.8334(5)
Co4: 6h (*x*,2*x*,1/4), *x*	0.8309(8)	0.8358(8)	0.8309(14)
Co5:12k (*x*,2*x*,*z*), *x*	0.8370(6)	0.8393(5)	0.8404(9)
z	0.0873(2)	0.0871(2)	0.0864(2)
R factors:			
R_{wp} (%)	8.81	9.39	8.97
R_p (%)	6.84	7.24	6.96
R_e (%)	5.22	4.86	6.97

3.2. Magnetic structure and magnetic properties

The parent compound Nd_2Co_7 experiences two spin-reorientation transitions as the temperature increases: one is at $T_{SR1}=218$ K and the other at $T_{SR2}=261$ K as shown in Fig. 4. This observation is consistent with the report of Andreev et al. [8] and Bartashevich et al. [9], showing that the easy magnetization direction of Nd_2Co_7 single crystal was along the *a*-axis below 225 K and along the *c*-axis above 290 K. In addition, the magnetization curve of Nd_2Co_7 mimics that of $NdCo_5$, implying a predominant contribution from the 1:5 slabs. The two spin-reorientation transitions are observed in the Fe substituted compounds $Nd_2Co_{7-x}Fe_x$ for $x<1.5$. However, the plateau defined as $\Delta T=T_{SR2}-T_{SR1}$ is narrowed with the increase of the Fe content and finally disappears for $x\geq 1.5$.

Fig. 5 shows the representative XRD patterns of the $Nd_2Co_{7-x}Fe_x$ fine powders magnetically aligned at room temperature in a field of ~10 kOe. For Nd_2Co_7 and samples with $x\leq 0.2$, the (0 0 l) reflections are strongly enhanced, indicating an easy magnetization direction (EMD) along the *c*-axis above T_{SR2} (>300 K). For the sample with $x\geq 0.8$, the (*h h* 0) reflections are strongly enhanced, implying that the EMD of the samples is planar at room temperature. For the samples with $0.4\leq x\leq 0.6$, the XRD patterns of the magnetically aligned powders are saliently different: both (0 0 l) and (*h h* 0) reflections are weakened while the (h0l) reflections are enhanced, implying the EMD of the sample at room temperature deviates from *c*-axis and *ab*-plane. Ilyn et al. have reported the anisotropy constants between 210 K and 270 K of Nd_2Co_7 that well reproduced the observed temperatures of the spin-reorientation transition [16]. From the reported anisotropy constants it is easy to derive that the EMD of Nd_2Co_7 alters rapidly from the *ab*-plane at T_{SR1} to the *c*-axis at T_{SR2} via a cone anisotropy. Considering $T_{SR1}<300\,K<T_{SR2}$ for the samples with $0.4\leq x\leq 0.6$

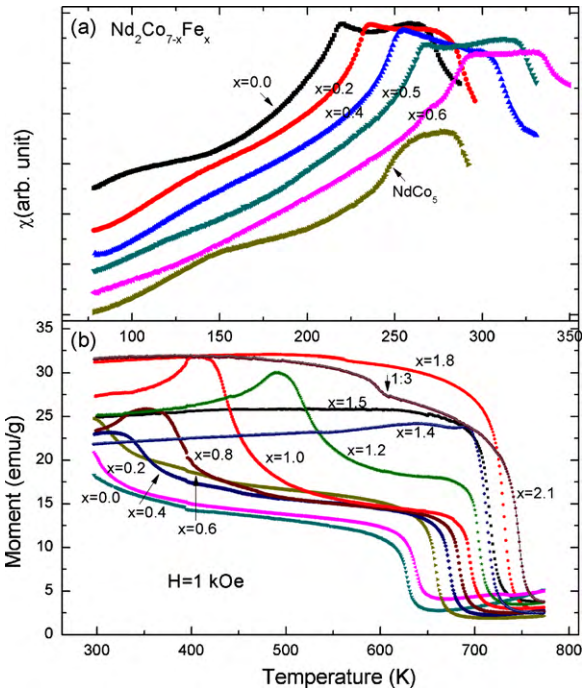

Fig. 4. Temperature dependence of ac susceptibility (a) and magnetization (b) of $Nd_2Co_{7-x}Fe_x$ compounds, the curve of $NdCo_5$ was measured and is presented for comparison. The arrow on $x = 2.1$ curve marks the Curie temperature of $Nd(CoFe)_3$ phase.

(Fig. 4), it is reasonable to infer that these compounds have a cone anisotropy at room temperature.

For both the Nd_2Co_7 and $NdCo_5$, the planar anisotropy of the Nd sublattice dominates at low temperature, while the *c*-axis anisotropy of the Co sublattice prevails at high temperature. The Stevens factors for the electronic configurations of Co and Fe have different signs in $R_{m+n}T_{2m+5n}$ series compounds [17]. Paoluzi et al. [18] also found that the overall anisotropy of Fe is not only 2–3 times larger than but also always opposite to that of Co in $Y_2(CoFe)_7$ compounds. In $Y(CoFe)_5$ structure, Franse et al. [19] reported that the anisotropy constant K_1s were 5.7×10^6 and -1.7×10^6 J/m^3 for Co in 2c and 3g sites, respectively, while those for Fe were almost one order of magnitude larger, i.e. -51.3×10^6 and 11.0×10^6 J/m^3,

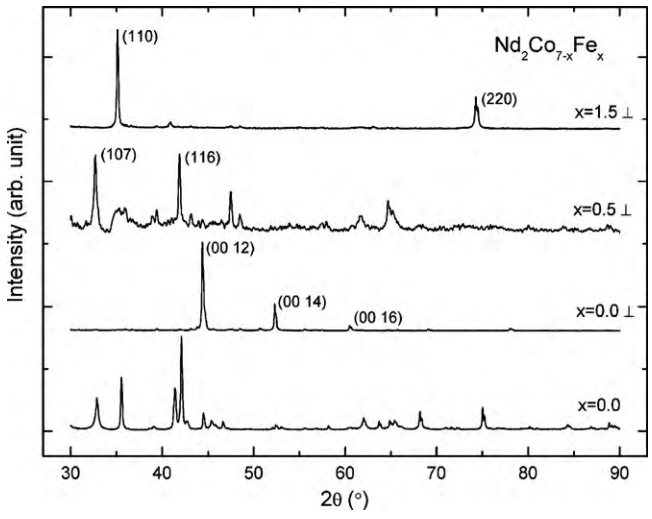

Fig. 5. The XRD patterns of magnetically pre-orientated powder sample of $Nd_2Co_{7-x}Fe_x$. The lowest curve is the XRD pattern of the un-orientated powder sample with $x = 0.0$.

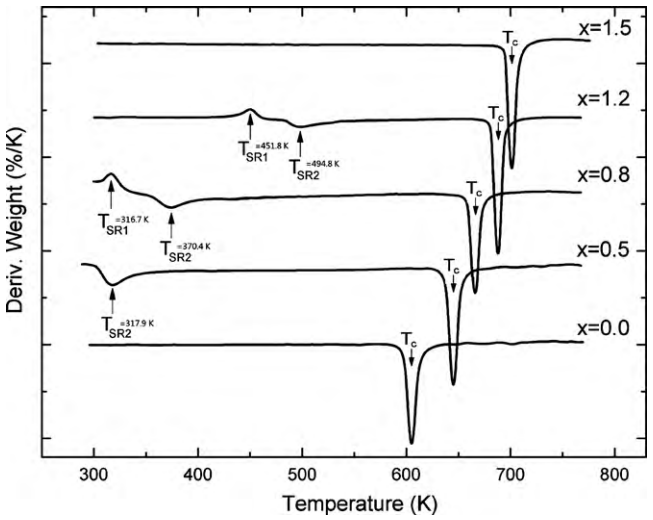

Fig. 6. Thermogravimetry traces under a low magnetic field for the $Nd_2Co_{7-x}Fe_x$.

respectively. The sign of the anisotropy of Fe in 2c site is opposite to and about five times larger than that in 3g site, which implies that a small amount of Fe in the 2c sites may offset the effect of the preferential substitution of Fe for Co in 3g sites. The 4e and 4f sites in the 2:7 structure, correspond to 2c sites in the 1:5 structure while the 6 h and 12k sites in the 2:7 structure to the 3g site in the 1:5 structure. Similarly, a small amount of Fe substitution for Co in the 4e and 4f sites could weaken the *c*-axis anisotropy of the transition metal sublattice in $Nd_2Co_{7-x}Fe_x$ substantially, giving rise to the enhancement of the planar anisotropy and the increase of the spin-reorientation temperature. For $x > 1.5$, the planar anisotropy dominates over the whole temperature range investigated, and no spin-reorientation transition takes place.

The spin-reorientation transition temperature and the Curie temperature of the compounds $Nd_2Co_{7-x}Fe_x$ can be readily determined by thermogravimetry analysis under a low magnetic field (Fig. 6) and ac susceptibility measurements (Fig. 4). The spin-reorientation transition and order–disorder magnetic transition (T_C) give rise to apparent weight-losses of a small piece of sample on the thermogravimetry trace under a low magnetic field exerted by a permanent magnet placed outside the furnace and on top of the crucible position. Based on these experiments and the XRD patterns of the magnetically aligned samples, the magnetic phase diagram is constructed as shown in Fig. 7 for the $Nd_2Co_{7-x}Fe_x$ compounds. It should be noted that the T_C derived from magnetization curves measured in 1 kOe (Fig. 4b) is about 15–20 K higher than that determined from thermogravimetry, probably due to temperature calibration of different apparatus and to the much higher magnetic field in the magnetization measurements. Fig. 7 indicates the spin-reorientation temperatures determined by thermogravimetry and ac susceptibility, both were performed under a low magnetic field, are coincident with each other.

The field dependence of magnetization of $Nd_2Co_{7-x}Fe_x$ compounds at 5 K is shown in Fig. 8, which was measured on fine particles by the SQUID magnetometer up to 70 kOe. All samples exhibit ferromagnetic character and tend to approach saturation in a field higher than 20 kOe. The saturation magnetization M_S are listed in Table 1 and displayed in Fig. 9. The M_S increases first gradually with the Fe content for $x \leq 0.20$, substantially for $0.20 < x < 1.5$, and then decreases for $x > 1.5$. Assuming the theoretical trivalent ion moment ($g_J\mu_B = 3.27\ \mu_B$) for Nd and a parallel alignment of the Nd moment and the Co moment, it is derived that the atomic moment of Co is 1.01 μ_B in Nd_2Co_7, which is close to the values in Y_2Co_7 ($\mu_{Co} = 1.06\ \mu_B$ [20]) and in La_2Co_7 ($\mu_{Co} = 1.06\ \mu_B$ [21,22]). Such a

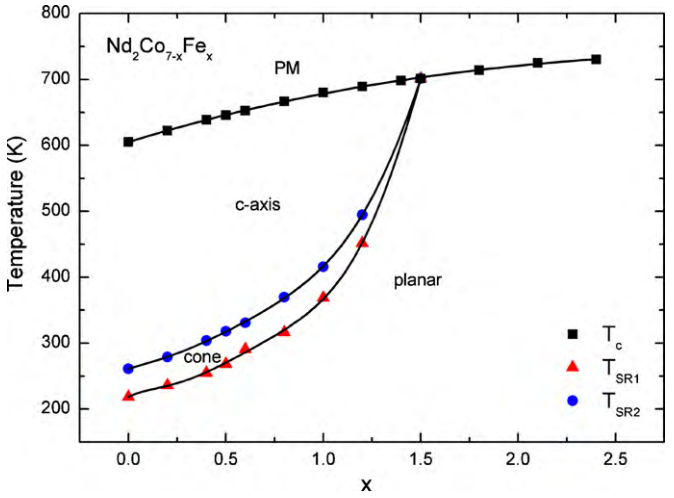

Fig. 7. Magnetic phase diagram of $Nd_2Co_{7-x}Fe_x$ compounds. The transition temperatures were derived from thermogravimetry and ac susceptibility measurements under a low field.

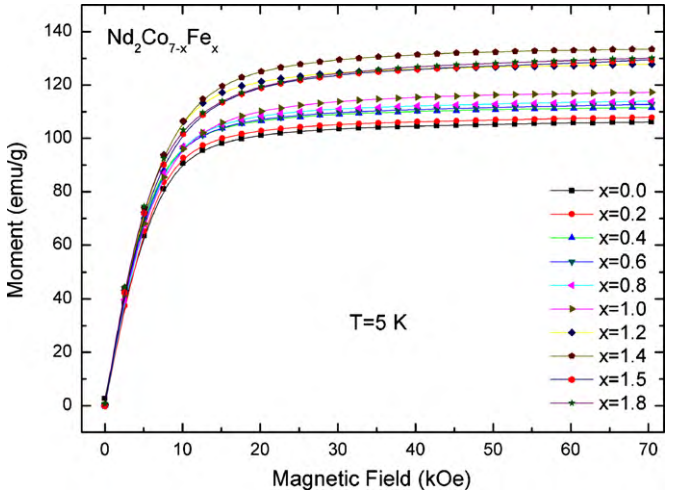

Fig. 8. The field dependence of magnetization of $Nd_2Co_{7-x}Fe_x$ compounds at 5 K.

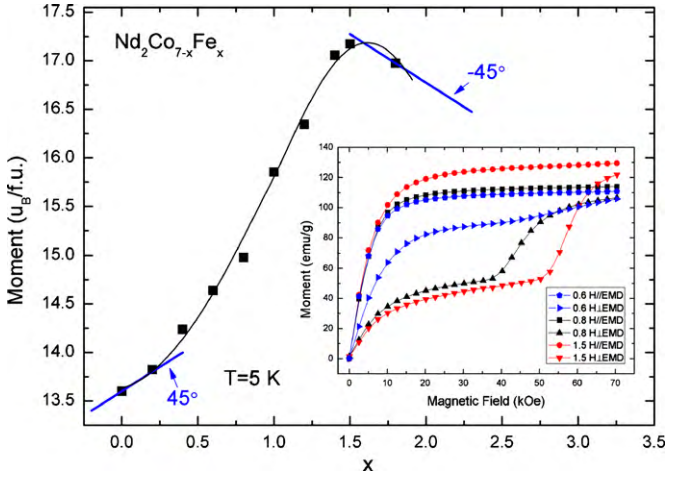

Fig. 9. Composition dependence of saturation moment of $Nd_2Co_{7-x}Fe_x$ compounds at 5 K. Inset: composition dependence of the magnetization at 5 K of the magnetically pre-aligned samples with $x = 0.6$, 0.8 and 1.5.

low atomic moment for Co implies the R_2Co_7 compounds (R = Nd, Y, La) are weak ferromagnetic within the scenario of the magnetic valence model [23–25]. Interestingly, for $x \leq 0.20$ the increase of the M_S seems to result essentially from the depletion of spin-down electrons due to the substitution of Fe for Co ($dM_S/dx = 1$). For the sample with $x = 1.5$, $\mu_{Co} = 1.52\,\mu_B$, which is close to the atomic moment of Co ($\mu_{Co} = 1.6\,\mu_B$) with strong ferromagnetism character [23–25]. Since the atomic moment of transition metal may be underestimated if the crystal-field effect on Nd moment is taken into account, the large atomic moment of the transition metal implies that the compound becomes strong ferromagnetism as the substitution of Fe for Co increases and consequently the reduction of the M_S for $x > 1.5$ can be attributed essentially to a depletion of the spin-up electrons, i.e. $dM_S/dx = -1$ as shown in Fig. 9. However, for the samples with $0.20 < x < 1.5$, the substantial increase of the M_S with the Fe content ($dM_S/dx \gg 1$ and is different from Fe–Co [26] binary alloys) could probably result from both the depletion of d electrons and a spin-flipping of electrons from spin-down to spin-up subband. The spin-flipping can occur when the splitting of the d band is increased due to the enhanced coupling between transition metal atoms, which is corroborated by the monotonous increase of the Curie temperature with the Fe content (Fig. 7).

In Fig. 9 the field dependence of magnetization at 5 K is shown in the inset for some samples perpendicularly aligned in a field of 10 kOe at room temperature. For the samples with $x = 0.8$ and 1.5, the EMD is unchanged upon cooling from room temperature to 5 K, and a field induced spin-reorientation or the first-order magnetization process (FOMP) occurs at 5 K when the applied magnetic field is perpendicular to the alignment direction, which may result in appreciable magnetocaloric effects. In contrast, the EMD of the sample with $x = 0.6$ changes to planar one at low temperature, so only a small upturn is observed when the applied magnetic field is perpendicular to the alignment direction. Since the FOMP phenomenon in unaligned bulk samples is very weak, the magnetocaloric effects of the bulk samples have not been further pursued.

4. Conclusions

In summary, single phase compounds $Nd_2Co_{7-x}Fe_x$ have been prepared with $x < 2.1$. The compounds crystallized in the Ce_2Ni_7-type structure with a space group $P6_3/mmc$. For $x > 2.1$ the $Nd_2(CoFe)_7$ either coexists with the $Nd(CoFe)_3$ phase or decomposes to $Nd(CoFe)_3 + Nd_2(CoFe)_{17}$ ($x > 2.4$). The lattice parameter a of the $Nd_2Co_{7-x}Fe_x$ increases with the Fe content. The thickness of the $Nd(CoFe)_5$ slabs along the c-axis expands while that of the $Nd(CoFe)_2$ sables shrinks, which leads to a slight decrease of the c-axis with the Fe content.

For $x < 1.5$, the $Nd_2Co_{7-x}Fe_x$ compounds experience two spin-reorientation transitions. The substitution of Fe for Co elevates both the spin-reorientation transition temperatures and finally leads to a single ferromagnetism to paramagnetism transition for $x \geq 1.5$. Based on magnetic measurements, thermogravimetry analysis and XRD on magnetically aligned samples, a magnetic phase diagram is constructed for the $Nd_2Co_{7-x}Fe_x$. The saturation magnetization M_S increases gradually first with the Fe content for $x \leq 0.20$, substantially for $0.20 < x < 1.5$, and then decreases for $x > 1.5$. The composition dependence of the M_S can be elucidated by a depletion effect of d band electrons due to the substitution of Fe for Co and the spin-flipping due to an enhanced d band splitting.

Acknowledgements

This work is supported by the National Natural Science Foundation of China (Grants No. 50631040) and the National

Basic Research Program of China (Grant No. 2006CB601101, 2006CB605101).

References

[1] E. Parthé, B. Chabot, in: K.A. Sschneidner Jr., L. Eyring (Eds.), Handbook on the Physics and Chemistry of Rare Earths, vol. 7, North-Holland, Amsterdam, 1984, p. 186.
[2] Y. Khan, Acta Crystallogr. B 30 (1974) 1533.
[3] K.H.J. Buschow, R.P. van Stapele, J. Appl. Phys. 41 (1970) 4066.
[4] V.K. Pecharsky, K.A. Gschneidner Jr., J. Magn. Magn. Mater. 200 (1999) 44.
[5] P.J. von Ranke, V.K. Pecharsky, K.A. Gschneidner Jr., Phys. Rev. B 58 (1998) 12110.
[6] P.J. von Ranke, N.A. de Oliveira, V.S.R. de Sousa, D.C. Garcia, I.G. de Oliveira, A. Magnus, G. Carvalho, S. Gama, J. Magn. Magn. Mater. 313 (2007) 176.
[7] J.C.P. Campoy, E.J.R. Plaza, A.A. Coelho, S. Gama, Phys. Rev. B 74 (2006) 134410.
[8] A.V. Andreev, M.I. Bartashevich, A.V. Deryagin, S.M. Zadvorkin, Ye. N. Tarasov, Phys. Met. Metallogr. 65 (1988) 61.
[9] M.I. Bartashevish, T. Goto, M. Yamaguchi, J. Magn. Magn. Mater. 111 (1992) 83.
[10] G.H. Rao, S. Wu, X.H. Yan, Y.L. Zhang, W.H. Tang, J.K. Liang, J. Alloys Compd. 202 (1993) 101.
[11] F. Izumi, T. Ikeda, Mater. Sci. Forum 321–323 (2000) 198.
[12] J.M. Alameda, D. Givord, C. Jeandey, H.S. Li, Q. Lu, J.L. Oddou, J. Phys. 46 (1985) 1581.
[13] J. Déportes, D. Givord, J. Schweizer, F. Tasset, IEEE Trans. Magn. 12 (1976) 1000.
[14] J. Laforest, J.S. Shah, IEEE Trans. Magn. 9 (1973) 217.
[15] C.C. Tang, W.S. Zhan, Y.X. Li, D.F. Chen, J. Du, G.H. Wu, Z.W. Gan, S.R. Qi, J. Phys. D: Appl. Phys. 31 (1998) 2426.
[16] M. Ilyn, A.V. Andreev, E.A. Tereshina, M.I. Bartashevich, V. Zhukova, A. Zhukov, J. Gonzalez, in: The 2009 International Magnetics (Intermag) Conference Sacramento, California, May 4–8, 2009.
[17] M.I. Bartashevich, T. Goto, K. Koui, Phys. B: Condens. Matter 292 (2000) 9.
[18] A. Paoluzi, L. Pareti, M. Solzi, F. Albertini, J. Magn. Magn. Mater. 132 (1994) 185.
[19] J.J.M. Franse, N.P. Thuy, N.M. Hong, J. Magn. Magn. Mater. 72 (1988) 361.
[20] E. Koen, J. Schweizer, F. Tasset, Phys. Rev. 186 (1969) 479.
[21] W.A.J.J. Velge, K.H.J. Buschow, J. Appl. Phys. 39 (1968) 1717.
[22] K.H.J. Buschow, J. Less Common Met. 33 (1973) 311.
[23] A.P. Malozemoff, A.R. Williams, V.L. Moruzzi, Phys. Rev. B 29 (1984) 1620.
[24] A.R. Williams, V.L. Moruzzi, A.P. Malozemoff, K. Terakura, IEEE Trans. Magn. 19 (1983) 1983.
[25] G.H. Rao, J. Magn. Magn. Mater. 139 (1995) 204.
[26] A. Díaz-Ortiz, R. Drautz, M. Fähnle, H. Dosch, J.M. Sanchez, Phys. Rev. B 73 (2006) 224208.